Am J Nucl Med Mol Imaging 2018;8(6):360-372
www.ajnmmi.us /ISSN:2160-8407/ajnmmi0087564

Review Article

Early perfusion and dopamine transporter imaging using ^{18}F-FP-CIT PET/CT in patients with parkinsonism

Chae-Moon Hong[1,3], Ho-Sung Ryu[2,4], Byeong-Cheol Ahn[1,3]

Departments of [1]Nuclear Medicine, [2]Neurology, Kyungpook National University Hospital, Daegu, Republic of Korea; Departments of [3]Nuclear Medicine, [4]Neurology, School of Medicine, Kyungpook National University, Daegu, Republic of Korea

Received October 30, 2018; Accepted December 3, 2018; Epub December 20, 2018; Published December 30, 2018

Abstract: Combined use of ^{18}F-N-(3-fluoropropyl)-2β-carboxymethoxy-3β-(4-iodophenyl)nortropane (FP-CIT) for dopamine transporter imaging and ^{18}F-fludeoxyglucose (FDG) for glucose metabolism shows good diagnostic performance for differential diagnosis of Parkinson disease (PD) and Parkinson plus syndrome (multiple system atrophy, progressive supranuclear palsy, corticobasal degeneration, and dementia with Lewy bodies). A recent study showed that ^{18}F-FP-CIT positron emission tomography (PET) with early perfusion imaging is useful for the differential diagnosis of PD and Parkinson plus syndrome with lower radiation exposure, time, and cost. In this review, we summarize the advantages of using ^{18}F-FP-CIT PET for perfusion and dopamine transporter imaging, as well as clinical features useful for the differential diagnosis of PD and Parkinson plus syndrome.

Keywords: FP-CIT, PET, dual-phase, perfusion, dopamine transporter, FDG, parkinsonism, parkinson plus syndrome

Introduction

Parkinsonism is a syndrome of movement disorders characterized by a combination of six cardinal features including, bradykinesia, rigidity, resting tremor, postural instability, flexed posture, and freezing [1]. Parkinsonism shows the highest frequency among referral movement disorders in the clinic, and the causes of parkinsonism are variable. Parkinson disease (PD) is the most common form of parkinsonism. Parkinson plus syndrome, such as multiple system atrophy (MSA), progressive supranuclear palsy (PSP), corticobasal degeneration (CBD), and dementia with Lewy bodies (DLB), is another cause of parkinsonism that should be distinguished from PD [2].

Parkinson plus syndrome exhibits the following additional neurological features: autonomic dysfunction and cerebellar ataxia in MSA; supranuclear ophthalmoparesis in PSP; a combination of dystonia, myoclonus, apraxia, cortical sensory deficit, and alien hand in CBD; and early, prominent dementia in DLB [3].

To date, the therapeutic strategies for these chronic neurodegenerative disorders are based on symptomatic treatments. Dopaminergic medications are well-known representative drugs and are remarkably effective for symptom relief in patients with PD [4]. In contrast, no effective treatment has been developed for patients with Parkinson plus syndrome, and the prognosis of patients with Parkinson plus syndrome is poorer than that of patients with PD [5]. Accurate differential diagnosis will help not only the clinician to determine treatment regimens and prognosis but also the patient to plan rest of their life. Recently, several clinical trials of patients with Parkinson plus syndrome have been conducted to investigate new therapeutic drugs, and the importance of achieving an accurate differential diagnosis in the early stage of Parkinson plus syndrome has been emphasized. As there are no reliable biomarkers for any of these disorders, the proposed clinical diagnostic criteria based on the presence of clinical features are used for differential diagnosis of parkinsonism. However, this condition is challenging to accurately diagnose because patients

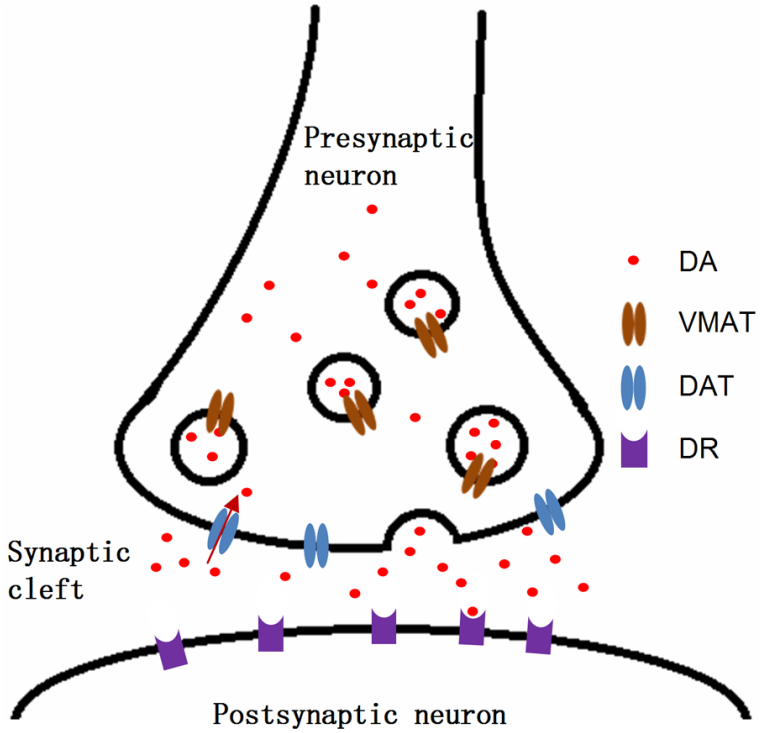

Figure 1. Schematic diagram of dopamine neuronal synapse in striatum. Nigrostriatal dopamine neuron releases the dopamine into the synaptic cleft in striatum, and the released dopamine binds to dopamine receptor in postsynaptic neuron. Dopamine transporters (DAT) on the membrane of presynaptic dopamine neuron reuptake the dopamine in synaptic cleft. Vesicular monoamine transporters (VMAT) transport the dopamine into the vesicles, and vesicles release dopamine to the synaptic cleft. DA, dopamine; VMAT, vesicular monoaminergic transporter; DAT, dopamine transporter; DR, dopamine receptor.

with parkinsonian disorders show similar symptoms, and distinct symptoms do not occur in the early stage [6].

Dopamine transporter imaging

To evaluate the presynaptic nigrostriatal dopamine neurons in striatum, positron emission tomography (PET) and single-photon emission computed tomography (SPECT) technology have been used since the 1980s. ^{18}F-dihydroxyphenylalanine (DOPA), which reflects aromatic L-amino acid decarboxylase (AADC) activity, was initially introduced, but there were several factors limiting its widespread use in clinics [7]. ^{18}F-DOPA PET is an indirect imaging method of the presynaptic nigrostriatal neurons, and some reports observed upregulation of AADC activity in patients with early PD [8]. Therefore, other targets for dopamine neurons were developed.

The terminals of nigrostriatal dopaminergic neurons express dopamine transporters (DAT), which are responsible for dopamine uptake from the synaptic cleft, making DAT a distinct molecular target (**Figure 1**) [9]. Recently, many radiotracers were developed to evaluate presynaptic DAT function: ^{123}I-2β-carbomethoxy-3β-(4-iodophenyl)tropane (β-CIT) (**Figure 2A**), ^{123}I-N-(3-fluoropropyl)-2β-carboxymethoxy-3β-(4-iodophenyl)nortropane (FP-CIT) (**Figure 2B**), ^{123}I-altropane, ^{99m}Tc-TRODAT for SPECT imaging, and ^{11}C-RTI 32, ^{11}C-CFT, ^{11}C-methylphenidate, ^{11}C-nomifensine, and ^{18}F-FP-CIT (**Figure 2C**) for PET imaging [9].

^{123}I-β-CIT shows a good striatal/cerebellar uptake ratio, but 24 h are required to equilibrate the tracer after intravenous injection [9]. ^{123}I-β-CIT also non-selectively binds to noradrenaline and serotonin transporters with a similar or lower nanomolar affinity [10]. Therefore, new tracers with better kinetics and DAT selectivity were developed. DAT imaging using ^{123}I-FP-CIT can be performed between 3 and 6 h after intravenous injection and shows better DAT selectivity than ^{123}I-β-CIT [11, 12]. DAT imaging using ^{123}I-FP-CIT is widely used and commercially available in Europe (since 2000) and the United States (since 2011). Several multicenter studies have evaluated the use of ^{123}I-FP-CIT [13, 14].

FP-CIT also can be labeled with ^{18}F for PET imaging without modifying the chemical structure. ^{18}F-FP-CIT has several advantages for DAT imaging compared to ^{123}I-FP-CIT. PET provides higher resolution than SPECT. The half-life of ^{18}F (109.8 min) is relatively longer than those of other PET radionuclides (e.g., ^{11}C), and ^{18}F is better for the production and commercialization of PET probes. One of the minor metabolites (<4%) of FP-CIT is nor-β-CIT, which is hydrophilic [15]. ^{123}I still labels nor-β-CIT, but ^{18}F is

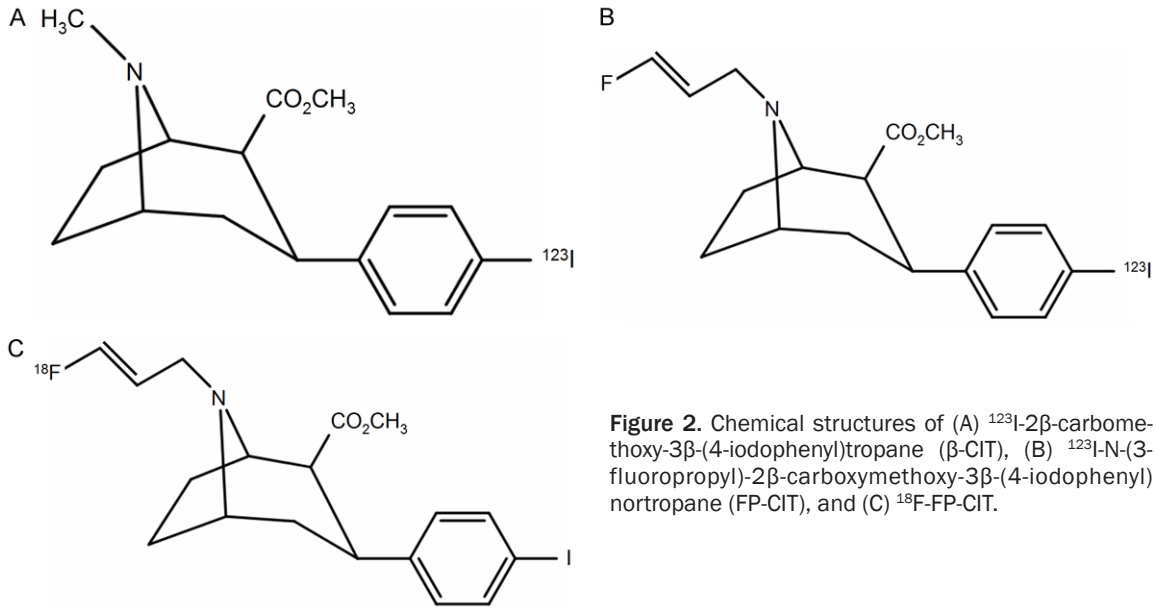

Figure 2. Chemical structures of (A) ^{123}I-2β-carbomethoxy-3β-(4-iodophenyl)tropane (β-CIT), (B) ^{123}I-N-(3-fluoropropyl)-2β-carboxymethoxy-3β-(4-iodophenyl) nortropane (FP-CIT), and (C) ^{18}F-FP-CIT.

detached from nor-β-CIT and converted to a hydrophilic metabolite. As nor-β-CIT can be taken up by the brain, ^{18}F-FP-CIT shows better kinetics than ^{123}I-FP-CIT [11]. A recent study comparing ^{123}I-FP-CIT and ^{18}F-FP-CIT showed that visual analyses using both methods did not affect diagnostic accuracy, while semi-quantitative analysis resulted in better contrast of ^{18}F-FP-CIT PET/CT relative to ^{123}I-FP-CIT SPECT/CT [16]. The low radiochemical yield of ^{18}F-FP-CIT was a major factor limiting its widespread clinical use; however, recent advancements in ^{18}F labeling methods of FP-CIT have resulted in high radiochemical yields (>50%) with high reproducibility, enabling ^{18}F-FP-CIT to be used clinically and commercially [17].

^{18}F-FP-CIT binding in the normal putamen decreases with aging at the rate of 5.3-6.4% per decade [11, 18], which is comparable to the results of multicenter studies examining healthy controls by ^{123}I-FP-CIT [13, 14]. ^{123}I-FP-CIT is not effective for differentiating PD from Parkinson plus syndrome [19], but ^{18}F-FP-CIT shows significant diagnostic value for the differentiation of not only PD but also Parkinson plus syndrome [20]. As PET provides higher anatomic resolution than SPECT, ^{18}F-FP-CIT can provide better regional characteristic features of PD, PSP, and MSA. Especially, decreased uptake of caudate nucleus in PSP and ventral putamen of MSA were reported using ^{18}F-FP-CIT PET/CT [20], but there is no report related to regional characteristics of Parkinsonism plus syndrome in ^{123}I-FP-CIT SPECT in our knowledge.

Perfusion imaging of ^{18}F-FP-CIT

^{18}F-FDG is the most commonly used radiotracer for assessing regional cerebral glucose metabolism as a marker of neuronal function. Previous studies and preliminary meta-analysis showed that ^{18}F-FDG PET is highly accurate (>90%) for distinguishing between PD and Parkinson plus syndrome [21]. As it is classically considered that cerebral blood flow and glucose metabolism are tightly coupled [22, 23], perfusion imaging can be used as an alternative to glucose imaging. A recent comparison study using ^{15}O-water for perfusion imaging and ^{18}F-FDG for glucose metabolism revealed some differences [22], that validating role of perfusion imaging for the differential diagnosis of Parkinson plus syndrome might be needed.

^{18}F-FP-CIT shows rapid increase of tracer uptake in brain with high extraction fraction rate after intravenous injection, which suggests that it has a high membrane permeability [11]. Early perfusion uptake of ^{18}F-FP-CIT in dopamine-poor regions (such as the cerebral cortex or cerebellum) shows peak around first 10 minutes after injection, DAT binding might be affected after 10 min [11, 24]. Therefore, early imaging within 10 min after intravenous injection of ^{18}F-FP-CIT well represents perfusion flow and mimics glucose metabolism in the brain, and several studies have been performed to

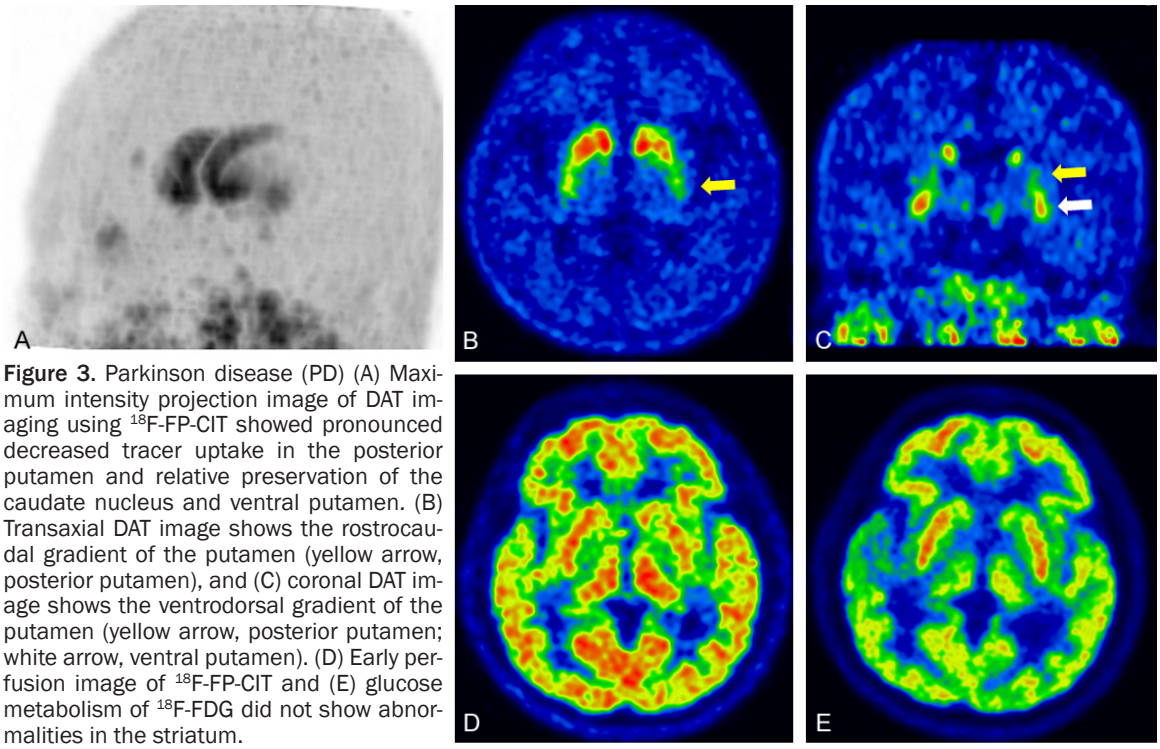

Figure 3. Parkinson disease (PD) (A) Maximum intensity projection image of DAT imaging using ^{18}F-FP-CIT showed pronounced decreased tracer uptake in the posterior putamen and relative preservation of the caudate nucleus and ventral putamen. (B) Transaxial DAT image shows the rostrocaudal gradient of the putamen (yellow arrow, posterior putamen), and (C) coronal DAT image shows the ventrodorsal gradient of the putamen (yellow arrow, posterior putamen; white arrow, ventral putamen). (D) Early perfusion image of ^{18}F-FP-CIT and (E) glucose metabolism of ^{18}F-FDG did not show abnormalities in the striatum.

evaluate the usefulness for perfusion imaging using ^{18}F-FP-CIT for the differential diagnosis of PD and Parkinson plus syndrome [24, 25]. However, perfusion images are typically obtained for 5-10 min after tracer injection, producing images with relatively lower quality than those obtained using ^{18}F-FDG, which hamper imaging interpretation in small regions such as the midbrain [24].

Differential diagnosis using ^{18}F-FP-CIT

Parkinson disease

Typical DAT images of PD show reduced tracer uptake in the putamen and caudate nucleus with a rostrocaudal gradient (anteroposterior gradient), and the caudate nucleus is less affected than the putamen [26]. These findings are well-known for DAT images using SPECT. As PET provides much higher resolution than SPECT, maximum intensity projection (MIP) images and coronal images are helpful for the differential diagnosis of parkinsonism. Not only the rostrocaudal gradient, but also the ventrodorsal gradient of putaminal DAT loss is a hallmark of PD in ^{18}F-FP-CIT images [20]. Therefore, PD patients show preserved DAT in the caudate nucleus and ventral putamen compared to in the posterior putamen. MIP images well visualize these characteristic findings of DAT images (**Figure 3**). As essential tremor or drug-induced parkinsonism shows normal DAT in the striatum, DAT imaging is very helpful for differentiating the causes of tremor from PD. Additionally, a recent study showed that lower DAT uptake may be related to the partial recovery of drug-induced parkinsonism [27]. However, it is difficult to differentiate PD from Parkinson plus syndrome using DAT images.

^{18}F-FDG PET scans of PD patients appear normal. Upon voxel-based statistical analyses and close inspection, PD is characterized by hypometabolism of the posterior temporoparietal, occipital cortex, and sometimes frontal cortex [21]. Perfusion images also show hypoperfusion in similar cortical regions [28]. From a clinical perspective, the role of early perfusion and metabolism imaging is more focused on the differential diagnosis of PD to Parkinson plus syndrome than on PD to normal cases.

Multiple system atrophy

MSA presents parkinsonian features of varying severity, cerebellar ataxia, autonomic failure, urogenital dysfunction, and corticospinal disor-

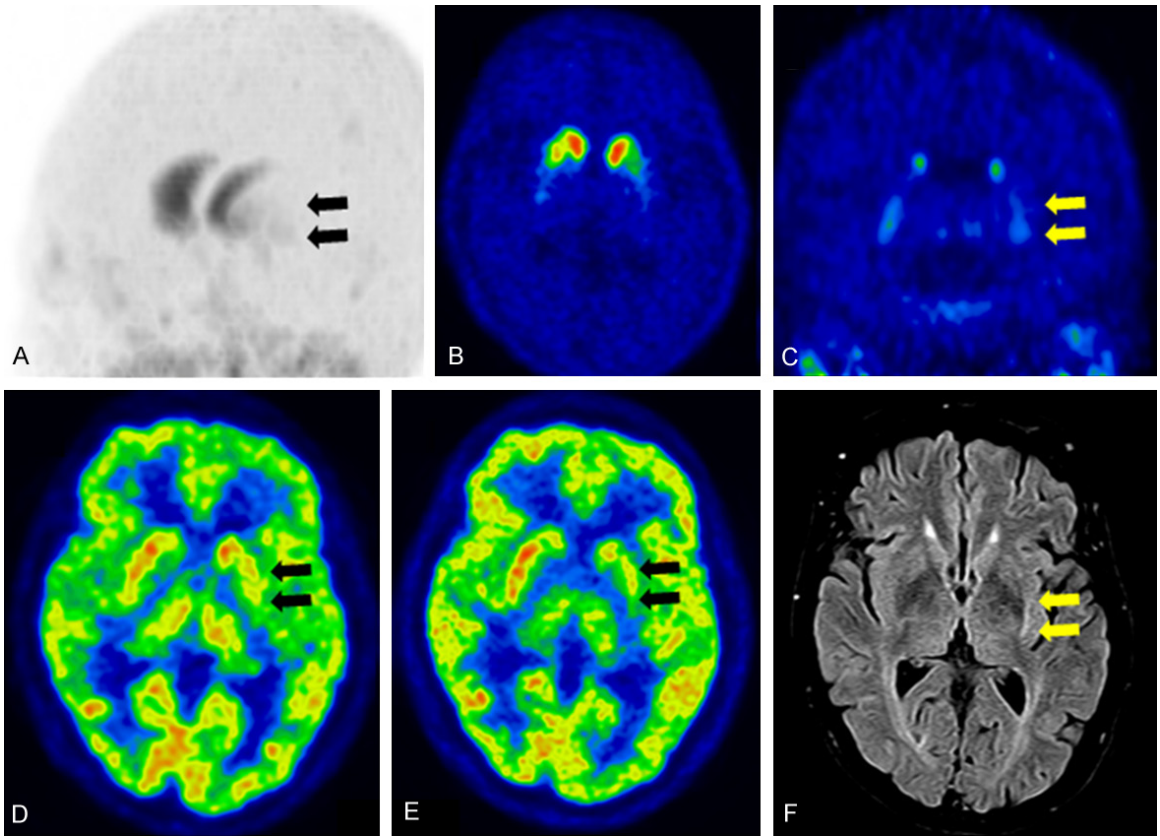

Figure 4. Multiple systemic atrophy with predominant parkinsonism (MSA-P) (A) Maximum intensity projection image of DAT imaging using ^{18}F-FP-CIT showing decreased tracer uptake in the posterior putamen and ventral putamen, and relative preservation of the caudate nucleus. (B) Transaxial DAT image showing decreased uptake of the putamen with the predominant left side, and (C) coronal DAT image showing equally decreased uptake in the dorsal and ventral putamen with loss of the ventrodorsal gradient. (D) Early perfusion image of ^{18}F-FP-CIT and (E) glucose metabolism of ^{18}F-FDG showing decreased perfusion and glucose hypometabolism in the posterior putamen. (F) FLAIR MR image showing atrophic changes in the left putamen and high signal intensity at the rim of the left putamen.

ders, and is divided into two categories: MSA with predominant parkinsonism (MSA-P) and MSA with predominant cerebellar ataxia (MSA-C) [29]. The 2008 consensus statement on the diagnosis of MSA includes ^{18}F-FDG and DAT imaging as additional features of possible MSA [30].

It is known that MSA-P patients are more predominantly affected by striatal DAT loss than MSA-C patients [26]. Kim et al. reported that all MSA-P patients showed striatal DAT loss, while 33% of MSA-C patients showed striatal DAT loss [31]. The higher resolution of PET using ^{18}F-FP-CIT enables discrimination of the ventral putamen and posterior putamen. MSA shows striatal DAT loss without a ventrodorsal gradient, with MSA suspected based on DAT images (**Figure 4**) [20]. However, the posterior putamen to ventral putamen ratio overlaps between patients with PD and MSA, making it difficult to establish a cut-off value of the ratio for differential diagnosis of PD and MSA. At the cutoff value for the ratio of the posterior putamen to ventral putamen (>0.65), sensitivity and specificity for differentiating MSA from PD were 90% and 45% respectively [20].

MSA shows decreased glucose metabolism at the striatum (particularly the posterior putamen) and cerebellum [21]. MSA-P patients showed decreased glucose metabolism at the striatum, with 50% of patients with MSA-P showing cerebellar hypometabolism. Patients with MSA-C showed decreased glucose metabolism at the cerebellum and 13% of patients with MSA-C showed striatal hypometabolism [31].

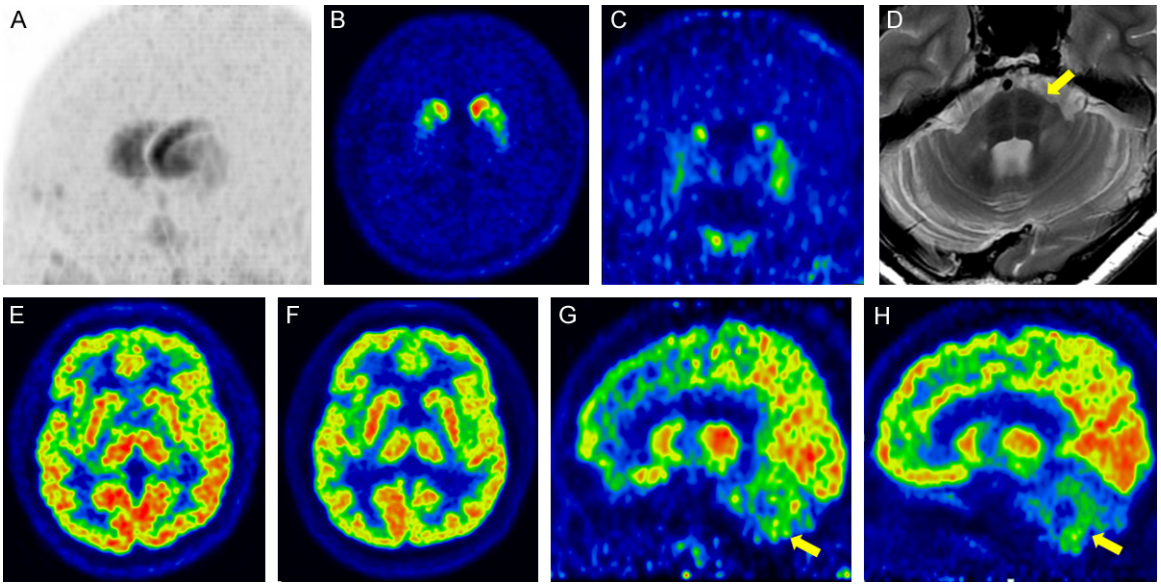

Figure 5. Multiple systemic atrophy with predominant cerebellar ataxia (MSA-C) (A) Maximum intensity projection image of DAT image using ^{18}F-FP-CIT showing decreased tracer uptake in the posterior putamen and ventral putamen, and relative preservation of the caudate nucleus. (B) Transaxial and (C) coronal DAT images showing decreased uptake in the dorsal and ventral putamen and loss of the ventrodorsal gradient. (D) Transaxial T2 MRI showing atrophic changes in the cerebellum and pons ("hot-cross bun sign", yellow arrow). (E) Transaxial early perfusion image of ^{18}F-FP-CIT and (F) glucose metabolism of ^{18}F-FDG showing no abnormality in the striatum. (G) Sagittal early perfusion imaging of ^{18}F-FP-CIT and (H) glucose metabolism of ^{18}F-FDG showing decreased perfusion and glucose hypometabolism in the cerebellum.

In early perfusion imaging using ^{18}F-FP-CIT, the cerebellum in MSA-C and putamen in MSA-P showed significant hypoperfusion compared to PD [25]. Particularly, MSA-C showed distinct hypoperfusion at the cerebellum compared to PD, resulting in clearer discrimination than ^{18}F-FDG [24]. In a comparison of putamen uptake between MSA-P and PD, perfusion images using ^{18}F-FP-CIT were less distinguishable than glucose metabolism using ^{18}F-FDG [24].

The designation of MSA-P or MSA-C refers to the predominant feature at the time the patient is evaluated, which can change over time [30]. Thus, predominant imaging features (such as DAT loss or cerebellar hypometabolism) are not used for the designation of MSA-P or MSA-C using current diagnostic criteria. However, combined interpretation of predominant clinical features and imaging finding is very helpful for diagnosing MSA subtypes. In patients with parkinsonian features without evident ataxia, demonstration of cerebellar hypometabolism or hypoperfusion can indicate a diagnosis of MSA-P rather than PD. In contrast, in the absence of parkinsonian features in a patient with cerebellar ataxia, evidence of DAT loss may point to the diagnosis of MSA-C (**Figure 5**) [32].

Progressive supranuclear palsy

The National Institute of Neurological Disorders and Stroke (NINDS) and Society for PSP (SPSP) international workshop proposed criteria for diagnosing classic PSP [33, 34]. The International Parkinson and Movement Disorder Society (MDS)-endorsed PSP Study Group provided revisions of the NINDS-SPSP criteria in 2017 [35]. Classic PSP, Richardson syndrome (PSP-RS), accounts for only 24% of 100 autopsy-confirmed PSP cases [36], and various subtypes of PSP have been proposed; initial predominance of ocular motor dysfunction (PSP-OM), postural instability (PSP-PI), Parkinsonism resembling idiopathic Parkinson disease (PSP-P), frontal lobe cognitive or behavioral presentations (PSP-F), including behavioral variant frontotemporal dementia (bvFTD), progressive gait freezing (PSP-PGF), corticobasal syndrome (PSP-CBS), primary lateral sclerosis (PSP-PLS), cerebellar ataxia (PSP-C), and speech/language disorders (PSP-SL), in-

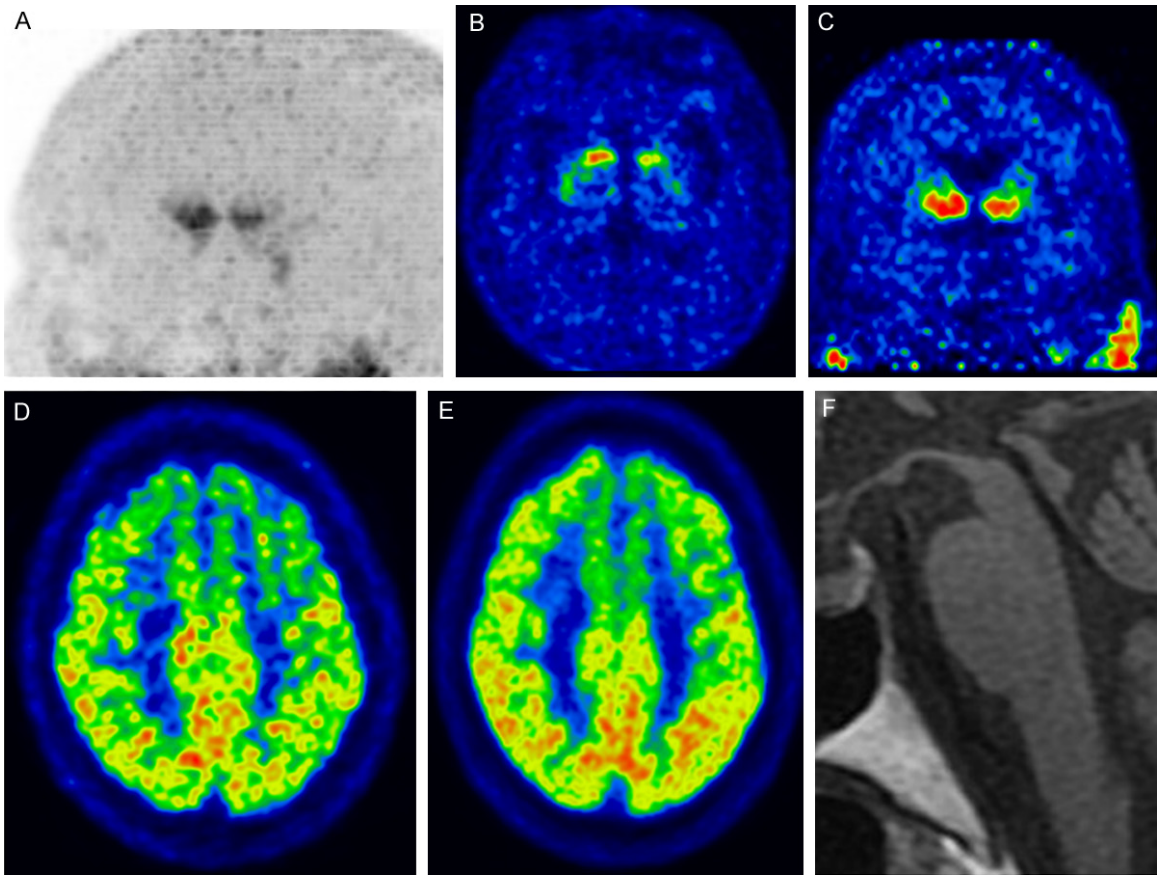

Figure 6. Progressive supranuclear palsy-Richardson syndrome (PSP-RS) (A) Maximum intensity projection image of DAT imaging using ^{18}F-FP-CIT showing prominently decreased tracer uptake in the caudate nucleus and decreased tracer uptake in the putamen. (B) Transaxial and (C) coronal DAT images showing decreased tracer uptake in both the anterior caudate nucleus (left dominant). (D) Early perfusion image of ^{18}F-FP-CIT and (E) glucose metabolism of ^{18}F-FDG showing decreased perfusion and glucose hypometabolism in the cerebellum. (F) Sagittal T1 MRI showing atrophic changes in the midbrain with preserved pons, known as the "hummingbird sign" or "penguin sign".

cluding nonfluent/agrammatic primary progressive aphasia (nfaPPA) and progressive apraxia of speech (AOS) [35].

DAT images show markedly reduced tracer uptake in the putamen and caudate nucleus (small rostrocaudal gradient and symmetric) in PSP-RS [26, 37], and the caudate nucleus is more affected than in PD [20, 24, 25, 38, 39]. Although advanced PD can show a decreased anterior caudate nucleus, the symptom duration of PSP would be much shorter than that of advanced PD because of the rapid progression of PSP [20]. The ratio of the anterior caudate to the ventral striatum showed excellent diagnostic value for differentiating PSP-RS from PD (cutoff, <0.7; sensitivity, 94%; specificity, 92%) [20]. Some studies did not show consistent diagnostic performance using caudate uptake [40, 41], but they performed analysis using ^{123}I-β-CIT SPECT, and the lower resolution may have affected the results. ^{18}F-FP-CIT PET shows higher resolution than SPECT and can clearly visualize decreased tracer uptake in the caudate nucleus (**Figure 6**). Additionally, midbrain tracer uptake is decreased in PSP-RS, with lower uptake than in PD but similar uptake as in MSA [42, 43]. Few studies have evaluated DAT imaging features in the other subtypes of non-PSP-RS [37]. PSP-PGF (also known as pure akinesia with gate freezing), PSP-P, and PSP-RS showed similar DAT imaging patterns of the striatum [37, 38, 44-46].

PSP-RS shows hypometabolism at the medial and dorsolateral frontal cortex, caudate nucleus, thalamus, and midbrain [21, 37] and greater frontal hypometabolism than in PD and MSA,

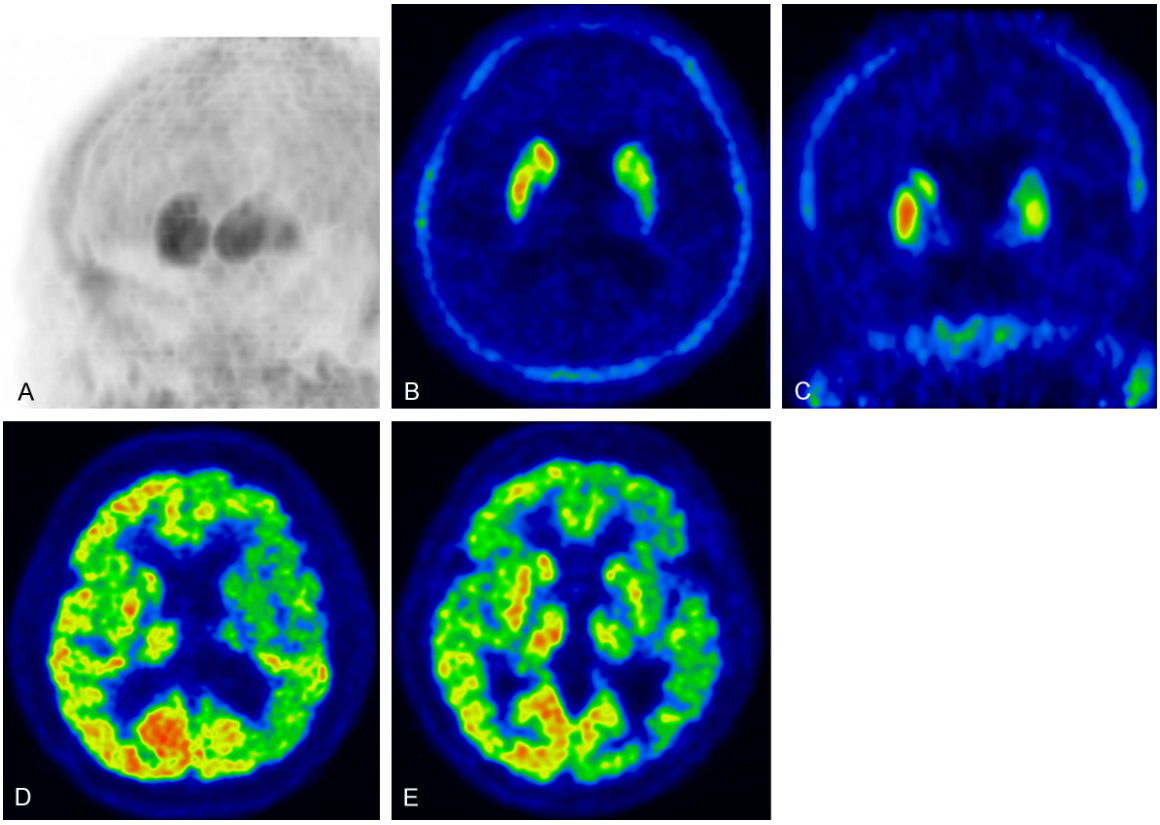

Figure 7. Corticobasal degeneration (CBD) (A) Maximum intensity projection image of DAT imaging using ^{18}F-FP-CIT showing prominent asymmetricity of the striatum. (B) Transaxial and (C) coronal DAT images showing decreased tracer uptake in the left caudate nucleus and putamen. (D) Early perfusion image of ^{18}F-FP-CIT and (E) glucose metabolism of ^{18}F-FDG showing decreased perfusion and glucose hypometabolism in the left cerebral hemisphere, striatum, and thalamus.

providing good diagnostic performance for diagnosing PSP-RS (sensitivity, 76%; specificity, 98%) [47, 48]. Early perfusion of ^{18}F-FP-CIT showed significant hypoperfusion in the medial frontal cortex compared to in MSA and PD, but not in the midbrain [24].

MDS-PSP criteria adopt only two imaging findings as supportive features: predominant midbrain atrophy or hypometabolism and postsynaptic striatal dopaminergic degeneration [35]. As current imaging techniques have not been compared to the neuropathological gold standard, the MDS-PSP criteria do not consider imaging features as strong evidence of PSP, and additional studies are needed to assess the value of these imaging studies [35, 37].

Corticobasal degeneration

CBD is a clinicopathologic entity, but various clinical features can occur in other pathologies, making differential diagnosis quite difficult [49]. The classic presentation with asymmetric rigidity, dystonia, and ideomotor apraxia is now referred to as corticobasal syndrome (CBS), but CBD has also been increasingly recognized to present with features that may overlap with frontotemporal lobe dementia, primary progressive aphasia, Alzheimer disease (AD), and PSP [3].

DAT images revealed reduced tracer uptake in the putamen and caudate nucleus (small rostrocaudal gradient), which mimics PSP; however, marked asymmetricity is a key feature of CBD compared to in PSP and MSA (**Figure 7**) [26]. Reduced FP-CIT uptake in patients with CBS was quite variable, and there was no significant correlation between tracer uptake values and clinical features such as disease duration and severity [50].

CBD is characterized by asymmetric hypometabolism of the frontoparietal areas, striatum, and thalamus [21]. Cortical hypometabolism

may be pronounced in the parietal cortex and typically extends across the sensorimotor cortex into the cingulate gyrus and premotor-to-posterior prefrontal areas [21]. Brain perfusion images can also be used to visualize asymmetric brain perfusion with similar patterns as ^{18}F-FDG [51, 52]. Additionally, as AD, PSP, CBD, and frontotemporal lobe dementia share tau pathology [53], characteristic metabolism and perfusion patterns of the diseases must be considered to ensure an accurate diagnosis.

Combined with pathologically confirmed CBD cases and consensus, 4 CBD phenotypes have been proposed: CBS, frontal behavioral-spatial syndrome, nonfluent/agrammatic variant of primary progressive aphasia, and PSP syndrome [49]. As the pathology of CBD is predicted antemortem in only 25-56% of cases [49], combined analysis of functional images and the subtypes of pathologic confirmed CBD are needed to increase the value of imaging studies.

Dementia with Lewy bodies

DLB is an early-onset rapidly progressive dementia that is part of the spectrum of PD [3]. The fourth consensus report of the DLB consortium considered the loss DAT imaging as an indicative biomarker and metabolism/perfusion change as a supportive biomarker [54].

DAT images of DLB showed decreased tracer uptake in the caudate nucleus and putamen. The rostrocaudal gradient in DLB may be flatter than in PD because of the relatively early involvement of the caudate nucleus [55, 56]. DAT imaging shows good diagnostic accuracy (86%) for distinguishing autopsy-confirmed DLB from AD [57]. Normal DAT uptake was reported in 10% of autopsy-confirmed DLB, and these patients showed synucleinopathy in the limbic and neocortical areas but minimal pathology was found in the substantia nigra [57].

Glucose hypometabolism of the occipital cortex is correlated with the visual neuropathy of DLB [54]. Additionally, widespread lateral frontal and temporoparietal glucose hypometabolism was observed [21]. As DLB does not involve the posterior cingulate, which is commonly involved in AD, the posterior cingulate island sign can be observed in DLB patients [58]. Many perfusion imaging analyses were performed to differentiate DLB, revealing a similar hypoperfusion pattern as ^{18}F-FDG [54].

Future perspectives

Recent advancements have enabled simultaneous acquisition of PET images and magnetic resonance imaging (MRI) data. Conducting ^{18}F-FP-CIT and MRI together reduces the radiation burden and acquisition time. Recently, comparison studies of ^{18}F-FP-CIT PET/CT and PET/MR were performed, which showed similar image quality for visual analysis [59, 60]. MRI has better image resolution, better anatomical correlation, and more optimal subregional analysis; FP-CIT imaging may be available using PET/MR. A recent study revealed a correlation between the binding ratio of ^{18}F-FP-CIT and gray matter density using PET/MR [61]. However, ^{18}F-FP-CIT PET/MR caused spatial bias in quantification, although attenuation maps accounted for cortical bones, and improvements in attenuation correction are needed for data comparison [59].

Recently, deep learning-based artificial intelligence (AI) has been widely applied in the medical imaging field [62]. Most of the characteristic imaging features can be detected by direct observation but applying deep learning-based AI might provide new imaging biomarkers for PD and Parkinson plus syndrome automatically. A recent study using deep-learning based AI effectively classified PD with ^{123}I-FP-CIT SPECT and classified clinical PD in patients whose scans showed no evidence of dopaminergic deficit [63]. However, deep-learning technology requires a large data set that relatively smaller number patients with Parkinson plus syndrome is a limiting factor, and difficulty in determining a definite diagnosis limit the application of this technology for diagnosing the disease. Multicenter pathologic-confirmed imaging data are required to use deep learning technology for disease analysis.

The other application of deep learning-based AI is for image reconstruction is to improve image quality [64]. Because of the limited time for acquisition (less than 10 min) of the perfusion phase using ^{18}F-FP-CIT, improvements in image quality are difficult to achieve using conventional reconstruction procedures. Recent image generation approaches using deep learning may be helpful for reconstructing perfusion

images, which is more practical in clinical practice.

Conclusion

^{18}F-FP-CIT PET with early perfusion and DAT imaging is useful for the differential diagnosis of PD and Parkinson plus syndrome (MSA, PSP, CBD, and DLB). Early perfusion images can be acquired with less radiation exposure, time, and cost. Further studies are needed to verify the results using autopsy-confirmed Parkinson plus syndromes and their subtypes.

Acknowledgements

This research was supported by a grant of the Korea Health Technology R&D Project through the Korea Health Industry Development Institute (KHIDI), funded by the Ministry of Health & Welfare, Republic of Korea (grant number: HI-15C0001).

Disclosure of conflict of interest

None.

Address correspondence to: Dr. Byeong-Cheol Ahn, Department of Nuclear Medicine, Kyungpook National University Hospital, 130 Dongdeok-ro, Jung Gu, Daegu 41944, Republic of Korea. Tel: 82-53-200-5583; Fax: 82-53-422-0864; E-mail: abc2000@knu.ac.kr

References

[1] Hughes AJ, Daniel SE and Lees AJ. The clinical features of Parkinson's disease in 100 histologically proven cases. Adv Neurol 1993; 60: 595-599.

[2] Bower JH, Dickson DW, Taylor L, Maraganore DM and Rocca WA. Clinical correlates of the pathology underlying parkinsonism: a population perspective. Mov Disord 2002; 17: 910-916.

[3] McFarland NR. Diagnostic approach to atypical parkinsonian syndromes. Continuum (Minneap Minn) 2016; 22: 1117-1142.

[4] Poewe W. Treatments for Parkinson disease--past achievements and current clinical needs. Neurology 2009; 72: S65-73.

[5] Fahn S, Jankovic J and Hallett M. Atypical parkinsonism, parkinsonism-plus syndromes, and secondary parkinsonian disorders. In: Fahn S, Jankovic J, Hallett M, editors. Principles and practicce of movement disorders. 2nd edition. Elsevier; 2001.

[6] Poewe W and Wenning G. The differential diagnosis of Parkinson's disease. Eur J Neurol 2002; 9 Suppl 3: 23-30.

[7] Kim JS, Oh SJ and Moon DH. Molecular imaging in neurodegenerative diseases. J Korean Med Assoc 2009; 52: 151-167.

[8] Lee CS, Samii A, Sossi V, Ruth TJ, Schulzer M, Holden JE, Wudel J, Pal PK, de la Fuente-Fernandez R, Calne DB and Stoessl AJ. In vivo positron emission tomographic evidence for compensatory changes in presynaptic dopaminergic nerve terminals in Parkinson's disease. Ann Neurol 2000; 47: 493-503.

[9] Brooks DJ. Molecular imaging of dopamine transporters. Ageing Res Rev 2016; 30: 114-121.

[10] Marek K, Innis R, van Dyck C, Fussell B, Early M, Eberly S, Oakes D and Seibyl J. [^{123}I]beta-CIT SPECT imaging assessment of the rate of Parkinson's disease progression. Neurology 2001; 57: 2089-2094.

[11] Kazumata K, Dhawan V, Chaly T, Antonini A, Margouleff C, Belakhlef A, Neumeyer J and Eidelberg D. Dopamine transporter imaging with fluorine-18-FPCIT and PET. J Nucl Med 1998; 39: 1521-1530.

[12] Djang DS, Janssen MJ, Bohnen N, Booij J, Henderson TA, Herholz K, Minoshima S, Rowe CC, Sabri O, Seibyl J, Van Berckel BN and Wanner M. SNM practice guideline for dopamine transporter imaging with ^{123}I-ioflupane SPECT 1.0. J Nucl Med 2012; 53: 154-163.

[13] Matsuda H, Murata M, Mukai Y, Sako K, Ono H, Toyama H, Inui Y, Taki Y, Shimomura H, Nagayama H, Tateno A, Ono K, Murakami H, Kono A, Hirano S, Kuwabara S, Maikusa N, Ogawa M, Imabayashi E, Sato N, Takano H, Hatazawa J and Takahashi R. Japanese multicenter database of healthy controls for [^{123}I]FP-CIT SPECT. Eur J Nucl Med Mol Imaging 2018; 45: 1405-1416.

[14] Varrone A, Dickson JC, Tossici-Bolt L, Sera T, Asenbaum S, Booij J, Kapucu OL, Kluge A, Knudsen GM, Koulibaly PM, Nobili F, Pagani M, Sabri O, Vander Borght T, Van Laere K and Tatsch K. European multicentre database of healthy controls for [^{123}I]FP-CIT SPECT (ENC-DAT): age-related effects, gender differences and evaluation of different methods of analysis. Eur J Nucl Med Mol Imaging 2013; 40: 213-227.

[15] Booij J and Kemp P. Dopamine transporter imaging with [^{123}I]FP-CIT SPECT: potential effects of drugs. Eur J Nucl Med Mol Imaging 2008; 35: 424-438.

[16] Lee I, Kim JS, Park JY, Byun BH, Park SY, Choi JH, Moon H, Kim JY, Lee KC, Chi DY, Kim KM, Lim I, Kang JH, Ahn SH, Kim BI, Ha JH and Lim SM. Head-to-head comparison of ^{18}F-FP-CIT

and ^{123}I-FP-CIT for dopamine transporter imaging in patients with Parkinson's disease: A preliminary study. Synapse 2018; 72: e22032.

[17] Lee SJ, Oh SJ, Chi DY, Kang SH, Kil HS, Kim JS and Moon DH. One-step high-radiochemical-yield synthesis of [^{18}F]FP-CIT using a protic solvent system. Nucl Med Biol 2007; 34: 345-351.

[18] Lee CS, Kim SJ, Oh SJ, Kim HO, Yun SC, Doudet D and Kim JS. Uneven age effects of [^{18}F]FP-CIT binding in the striatum of Parkinson's disease. Ann Nucl Med 2014; 28: 874-879.

[19] Isaias IU, Marotta G, Pezzoli G, Sabri O and Hesse S. [^{123}I]FP-CIT SPECT in atypical degenerative parkinsonism. Imaging in Medicine 2012; 4: 411-421.

[20] Oh M, Kim JS, Kim JY, Shin KH, Park SH, Kim HO, Moon DH, Oh SJ, Chung SJ and Lee CS. Subregional patterns of preferential striatal dopamine transporter loss differ in Parkinson disease, progressive supranuclear palsy, and multiple-system atrophy. J Nucl Med 2012; 53: 399-406.

[21] Meyer PT, Frings L, Rucker G and Hellwig S. ^{18}F-FDG PET in parkinsonism: differential diagnosis and evaluation of cognitive impairment. J Nucl Med 2017; 58: 1888-1898.

[22] Gur RC, Ragland JD, Reivich M, Greenberg JH, Alavi A and Gur RE. Regional differences in the coupling between resting cerebral blood flow and metabolism may indicate action preparedness as a default state. Cereb Cortex 2009; 19: 375-382.

[23] Sokoloff L. Relationships among local functional activity, energy metabolism, and blood flow in the central nervous system. Fed Proc 1981; 40: 2311-2316.

[24] Jin S, Oh M, Oh SJ, Oh JS, Lee SJ, Chung SJ and Kim JS. Additional value of early-phase ^{18}F-FP-CIT PET image for differential diagnosis of atypical parkinsonism. Clin Nucl Med 2017; 42: e80-e87.

[25] Jin S, Oh M, Oh SJ, Oh JS, Lee SJ, Chung SJ, Lee CS and Kim JS. Differential diagnosis of parkinsonism using dual-phase F-18 FP-CIT PET imaging. Nucl Med Mol Imaging 2013; 47: 44-51.

[26] Meyer PT and Hellwig S. Update on SPECT and PET in parkinsonism - part 1: imaging for differential diagnosis. Curr Opin Neurol 2014; 27: 390-397.

[27] Hong JY, Sunwoo MK, Oh JS, Kim JS, Sohn YH and Lee PH. Persistent drug-induced parkinsonism in patients with normal dopamine transporter imaging. PLoS One 2016; 11: e0157410.

[28] Borghammer P. Perfusion and metabolism imaging studies in Parkinson's disease. Dan Med J 2012; 59: B4466.

[29] Gilman S, Low PA, Quinn N, Albanese A, Ben-Shlomo Y, Fowler CJ, Kaufmann H, Klockgether T, Lang AE, Lantos PL, Litvan I, Mathias CJ, Oliver E, Robertson D, Schatz I and Wenning GK. Consensus statement on the diagnosis of multiple system atrophy. J Neurol Sci 1999; 163: 94-98.

[30] Gilman S, Wenning GK, Low PA, Brooks DJ, Mathias CJ, Trojanowski JQ, Wood NW, Colosimo C, Durr A, Fowler CJ, Kaufmann H, Klockgether T, Lees A, Poewe W, Quinn N, Revesz T, Robertson D, Sandroni P, Seppi K and Vidailhet M. Second consensus statement on the diagnosis of multiple system atrophy. Neurology 2008; 71: 670-676.

[31] Kim HW, Kim JS, Oh M, Oh JS, Lee SJ, Oh SJ, Chung SJ and Lee CS. Different loss of dopamine transporter according to subtype of multiple system atrophy. Eur J Nucl Med Mol Imaging 2016; 43: 517-525.

[32] Gilman S, Frey KA, Koeppe RA, Junck L, Little R, Vander Borght TM, Lohman M, Martorello S, Lee LC, Jewett DM and Kilbourn MR. Decreased striatal monoaminergic terminals in olivopontocerebellar atrophy and multiple system atrophy demonstrated with positron emission tomography. Ann Neurol 1996; 40: 885-892.

[33] Litvan I, Agid Y, Calne D, Campbell G, Dubois B, Duvoisin RC, Goetz CG, Golbe LI, Grafman J, Growdon JH, Hallett M, Jankovic J, Quinn NP, Tolosa E and Zee DS. Clinical research criteria for the diagnosis of progressive supranuclear palsy (Steele-Richardson-Olszewski syndrome): report of the NINDS-SPSP international workshop. Neurology 1996; 47: 1-9.

[34] Litvan I, Hauw JJ, Bartko JJ, Lantos PL, Daniel SE, Horoupian DS, McKee A, Dickson D, Bancher C, Tabaton M, Jellinger K and Anderson DW. Validity and reliability of the preliminary NINDS neuropathologic criteria for progressive supranuclear palsy and related disorders. J Neuropathol Exp Neurol 1996; 55: 97-105.

[35] Hoglinger GU, Respondek G, Stamelou M, Kurz C, Josephs KA, Lang AE, Mollenhauer B, Muller U, Nilsson C, Whitwell JL, Arzberger T, Englund E, Gelpi E, Giese A, Irwin DJ, Meissner WG, Pantelyat A, Rajput A, van Swieten JC, Troakes C, Antonini A, Bhatia KP, Bordelon Y, Compta Y, Corvol JC, Colosimo C, Dickson DW, Dodel R, Ferguson L, Grossman M, Kassubek J, Krismer F, Levin J, Lorenzl S, Morris HR, Nestor P, Oertel WH, Poewe W, Rabinovici G, Rowe JB, Schellenberg GD, Seppi K, van Eimeren T, Wenning GK, Boxer AL, Golbe LI, Litvan I; Movement Disorder Society-endorsed PSPSG. Clinical diagnosis of progressive supranuclear palsy: the

movement disorder society criteria. Mov Disord 2017; 32: 853-864.
[36] Respondek G, Stamelou M, Kurz C, Ferguson LW, Rajput A, Chiu WZ, van Swieten JC, Troakes C, Al Sarraj S, Gelpi E, Gaig C, Tolosa E, Oertel WH, Giese A, Roeber S, Arzberger T, Wagenpfeil S, Höglinger GU; Movement Disorder Society-endorsed PSP Study Group. The phenotypic spectrum of progressive supranuclear palsy: a retrospective multicenter study of 100 definite cases. Mov Disord 2014; 29: 1758-1766.
[37] Whitwell JL, Hoglinger GU, Antonini A, Bordelon Y, Boxer AL, Colosimo C, van Eimeren T, Golbe LI, Kassubek J, Kurz C, Litvan I, Pantelyat A, Rabinovici G, Respondek G, Rominger A, Rowe JB, Stamelou M, Josephs KA; Movement Disorder Society-endorsed PSPSG. Radiological biomarkers for diagnosis in PSP: where are we and where do we need to be? Mov Disord 2017; 32: 955-971.
[38] Han S, Oh M, Oh JS, Lee SJ, Oh SJ, Chung SJ, Park HK and Kim JS. Subregional pattern of striatal dopamine transporter loss on 18F FP-CIT positron emission tomography in patients with pure akinesia with gait freezing. JAMA Neurol 2016; 73: 1477-1484.
[39] Im JH, Chung SJ, Kim JS and Lee MC. Differential patterns of dopamine transporter loss in the basal ganglia of progressive supranuclear palsy and Parkinson's disease: analysis with [^{123}I]IPT single photon emission computed tomography. J Neurol Sci 2006; 244: 103-109.
[40] Pirker W, Asenbaum S, Bencsits G, Prayer D, Gerschlager W, Deecke L and Brucke T. [^{123}I] beta-CIT SPECT in multiple system atrophy, progressive supranuclear palsy, and corticobasal degeneration. Mov Disord 2000; 15: 1158-1167.
[41] Van Laere K, Casteels C, De Ceuninck L, Vanbilloen B, Maes A, Mortelmans L, Vandenberghe W, Verbruggen A and Dom R. Dual-tracer dopamine transporter and perfusion SPECT in differential diagnosis of parkinsonism using template-based discriminant analysis. J Nucl Med 2006; 47: 384-392.
[42] Goebel G, Seppi K, Donnemiller E, Warwitz B, Wenning GK, Virgolini I, Poewe W and Scherfler C. A novel computer-assisted image analysis of [^{123}I]beta-CIT SPECT images improves the diagnostic accuracy of parkinsonian disorders. Eur J Nucl Med Mol Imaging 2011; 38: 702-710.
[43] Seppi K, Scherfler C, Donnemiller E, Virgolini I, Schocke MF, Goebel G, Mair KJ, Boesch S, Brenneis C, Wenning GK and Poewe W. Topography of dopamine transporter availability in progressive supranuclear palsy: a voxelwise [^{123}I]beta-CIT SPECT analysis. Arch Neurol 2006; 63: 1154-1160.
[44] Fasano A, Baldari S, Di Giuda D, Paratore R, Piano C, Bentivoglio AR, Girlanda P and Morgante F. Nigro-striatal involvement in primary progressive freezing gait: insights into a heterogeneous pathogenesis. Parkinsonism Relat Disord 2012; 18: 578-584.
[45] Lin WY, Lin KJ, Weng YH, Yen TC, Shen LH, Liao MH and Lu CS. Preliminary studies of differential impairments of the dopaminergic system in subtypes of progressive supranuclear palsy. Nucl Med Commun 2010; 31: 974-980.
[46] Park HK, Kim JS, Im KC, Oh SJ, Kim MJ, Lee JH, Chung SJ and Lee MC. Functional brain imaging in pure akinesia with gait freezing: [^{18}F] FDG PET and [^{18}F] FP-CIT PET analyses. Mov Disord 2009; 24: 237-245.
[47] Klein RC, de Jong BM, de Vries JJ and Leenders KL. Direct comparison between regional cerebral metabolism in progressive supranuclear palsy and Parkinson's disease. Mov Disord 2005; 20: 1021-1030.
[48] Tripathi M, Dhawan V, Peng S, Kushwaha S, Batla A, Jaimini A, D'Souza MM, Sharma R, Saw S and Mondal A. Differential diagnosis of parkinsonian syndromes using F-18 fluorodeoxyglucose positron emission tomography. Neuroradiology 2013; 55: 483-492.
[49] Armstrong MJ, Litvan I, Lang AE, Bak TH, Bhatia KP, Borroni B, Boxer AL, Dickson DW, Grossman M, Hallett M, Josephs KA, Kertesz A, Lee SE, Miller BL, Reich SG, Riley DE, Tolosa E, Troster AI, Vidailhet M and Weiner WJ. Criteria for the diagnosis of corticobasal degeneration. Neurology 2013; 80: 496-503.
[50] Cilia R, Rossi C, Frosini D, Volterrani D, Siri C, Pagni C, Benti R, Pezzoli G, Bonuccelli U, Antonini A and Ceravolo R. Dopamine transporter SPECT imaging in corticobasal syndrome. PLoS One 2011; 6: e18301.
[51] Okuda B, Tachibana H, Kawabata K, Takeda M and Sugita M. Comparison of brain perfusion in corticobasal degeneration and Alzheimer's disease. Dement Geriatr Cogn Disord 2001; 12: 226-231.
[52] Hossain AK, Murata Y, Zhang L, Taura S, Saitoh Y, Mizusawa H, Oda K, Matsushima E, Okubo Y and Shibuya H. Brain perfusion SPECT in patients with corticobasal degeneration: analysis using statistical parametric mapping. Mov Disord 2003; 18: 697-703.
[53] Murray ME, Kouri N, Lin WL, Jack CR Jr, Dickson DW and Vemuri P. Clinicopathologic assessment and imaging of tauopathies in neurodegenerative dementias. Alzheimers Res Ther 2014; 6: 1.
[54] McKeith IG, Boeve BF, Dickson DW, Halliday G, Taylor JP, Weintraub D, Aarsland D, Galvin J, Attems J, Ballard CG, Bayston A, Beach TG, Blanc F, Bohnen N, Bonanni L, Bras J, Brundin P, Burn D, Chen-Plotkin A, Duda JE, El-Agnaf O, Feldman H, Ferman TJ, Ffytche D, Fujishiro H, Galasko D, Goldman JG, Gomperts SN, Graff-

Radford NR, Honig LS, Iranzo A, Kantarci K, Kaufer D, Kukull W, Lee VM, Leverenz JB, Lewis S, Lippa C, Lunde A, Masellis M, Masliah E, McLean P, Mollenhauer B, Montine TJ, Moreno E, Mori E, Murray M, O'Brien JT, Orimo S, Postuma RB, Ramaswamy S, Ross OA, Salmon DP, Singleton A, Taylor A, Thomas A, Tiraboschi P, Toledo JB, Trojanowski JQ, Tsuang D, Walker Z, Yamada M and Kosaka K. Diagnosis and management of dementia with Lewy bodies: fourth consensus report of the DLB Consortium. Neurology 2017; 89: 88-100.

[55] Booij J, Dubroff J, Pryma D, Yu J, Agarwal R, Lakhani P and Kuo PH. Diagnostic performance of the visual reading of ^{123}I-Ioflupane SPECT images with or without quantification in patients with movement disorders or dementia. J Nucl Med 2017; 58: 1821-1826.

[56] O'Brien JT, Colloby S, Fenwick J, Williams ED, Firbank M, Burn D, Aarsland D and McKeith IG. Dopamine transporter loss visualized with FP-CIT SPECT in the differential diagnosis of dementia with Lewy bodies. Arch Neurol 2004; 61: 919-925.

[57] Thomas AJ, Attems J, Colloby SJ, O'Brien JT, McKeith I, Walker R, Lee L, Burn D, Lett DJ and Walker Z. Autopsy validation of ^{123}I-FP-CIT dopaminergic neuroimaging for the diagnosis of DLB. Neurology 2017; 88: 276-283.

[58] O'Brien JT, Firbank MJ, Davison C, Barnett N, Bamford C, Donaldson C, Olsen K, Herholz K, Williams D and Lloyd J. ^{18}F-FDG PET and perfusion SPECT in the diagnosis of Alzheimer and Lewy body dementias. J Nucl Med 2014; 55: 1959-1965.

[59] Choi H, Cheon GJ, Kim HJ, Choi SH, Lee JS, Kim YI, Kang KW, Chung JK, Kim EE and Lee DS. Segmentation-based MR attenuation correction including bones also affects quantitation in brain studies: an initial result of ^{18}F-FP-CIT PET/MR for patients with parkinsonism. J Nucl Med 2014; 55: 1617-1622.

[60] Kwon S, Chun K, Kong E and Cho I. Comparison of the performances of ^{18}F-FP-CIT brain PET/MR and simultaneous PET/CT: a preliminary study. Nucl Med Mol Imaging 2016; 50: 219-227.

[61] Choi H, Cheon GJ, Kim HJ, Choi SH, Kim YI, Kang KW, Chung JK, Kim EE and Lee DS. Gray matter correlates of dopaminergic degeneration in Parkinson's disease: a hybrid PET/MR study using ^{18}F-FP-CIT. Hum Brain Mapp 2016; 37: 1710-1721.

[62] Choi H. Deep learning in nuclear medicine and molecular imaging: current perspectives and future directions. Nucl Med Mol Imaging 2018; 52: 109-118.

[63] Choi H, Ha S, Im HJ, Paek SH and Lee DS. Refining diagnosis of Parkinson's disease with deep learning-based interpretation of dopamine transporter imaging. Neuroimage Clin 2017; 16: 586-594.

[64] Zhu B, Liu JZ, Cauley SF, Rosen BR and Rosen MS. Image reconstruction by domain-transform manifold learning. Nature 2018; 555: 487-492.